CILAMCE 2017
Florianópolis - Santa Catarina - Brazil

ISOGEOMETRIC ANALYSIS APPLIED TO 2D CURVED BEAM ELEMENTS

Gianluca Marchiori

Alfredo Gay Neto

gianluca.marchiori@usp.br

alfredo.gay@usp.br

Polytechnic School at University of São Paulo

Av. Prof. Almeida Prado, 83, 05508-900, São Paulo, Brazil

Abstract. *Isogeometric analysis consists on building the exact geometry of the computational model with functions created by Computer Aided Design (CAD) technologies, such as B-Splines, NURBS (Non-Uniform Rational B-Splines) and T-Splines. Then, isoparametric concept is claimed, that is, the solution space is represented by means of the same functions used to describe the geometry. The Isogeometric concept was proposed by Hughes et al. (2005) and corresponds to the combination of Isoparametric analysis of finite elements with CAD description of geometry. Due to the easiness in generating the exact geometry of the model through CAD technologies, there are several works about isogeometric analysis being done. In this context, the aim of the present contribution is the study of isogeometric analysis applied to 2D beams. It begins with a description of CAD technologies used to describe the geometry, such as B-Splines and NURBS. Then, two formulations of isogeometric curved planar beam models are proposed, based on assumptions of Bernoulli-Euler and Timoshenko beams. Some examples of applications are presented and results are compared with analytical solutions, showing good agreement.*

Keywords: *Isogeometric analysis, Splines, Beam, Finite element method*

1 INTRODUCTION

Isogeometric analysis consists on building the exact geometry of the computational model with functions created by Computer Aided Design (CAD) technologies, such as B-Splines, NURBS (Non-Uniform Rational B-Splines) and T-Splines. Then, isoparametric concept is claimed, that is, the solution space is represented by means of the same basis (functions) used to describe the geometry. The isogeometric concept was proposed by Hughes *et al.* (2005) and corresponds to the combination of isoparametric analysis of finite elements with CAD description of geometry.

Isogeometric concept can be applied to problems governed by partial differential equations, such as solid and fluid mechanics, and has much in common with the finite element method. However, it is more geometric-based and straightforward to describe problems involving curved structures and surfaces, because of its inspiration in CAD. An important feature of isogeometric analysis using B-Splines and NURBS lies in the assurance of C^{p-1} continuity, where p is the order of the spline, as opposed to the C^0 continuity obtained through the traditional finite element method, by means of interpolation with Lagrange polynomials.

Due to the easiness in generating the exact geometry of the model through CAD technologies, there are several works about isogeometric analysis being done. The first publication on that corresponds to Hughes *et al.* (2005), in which the concept of isogeometric analysis was introduced. In Hughes *et al.* (2005), basis functions generated from NURBS are employed to construct exact geometric models. Refinements schemes are presented, such as h- and p-refinements, analogues to the finite element refinements, and third one (and elected as more efficient), so called k-refinement. Through these techniques, the basis functions used to define the geometry can be systematically enriched without altering the geometry or its parametrization. This means that adaptive mesh refinement techniques can be utilized without a link to the CAD (computer aided design) database, in contrast with finite element methods. In addition, examples of applications in structural and fluid analysis are made, and it is argued that isogeometric analysis is a viable alternative to standard, polynomial-based, finite element analysis.

One issue that affects efficiency corresponds to numerical quadrature and this was studied by Hughes *et al.* (2008). The authors arrived to a thumb rule called “half-point rule”, which indicates that optimal rules involve a number of points roughly equal to haft the number of degrees of freedom, or equivalently half the number of basis functions of the space under consideration. In addition, several rules of practical interest and a numerical procedure for determining efficient rules are presented.

With respect to beams, which correspond to the object of study of the present work, isogeometric analysis is present in several types of applications. In Cazzani *et al.* (2014) and Cazzani *et al.* (2015), 2D beam models are developed using NURBS to describe geometry and to interpolate displacements to be applied on problems involving curved beams and arcs. Another application of the isogeometric analysis corresponds to the study of beam vibrations, presented in Lee (2013) and Weeger (2013). Studies on the control of locking effects, such as shear locking, are presented by Beirão da Veiga *et al.* (2012), Auricchio *et al.* (2013) and Bouclier *et al.* (2012).

In this context, the aim of the present contribution is the study of isogeometric analysis applied to 2D beams. It begins with a description of CAD technologies used to describe the geometry, such as B-Splines and NURBS. Then, two formulations of isogeometric curved planar beam models are proposed, based on assumptions of Bernoulli-Euler and Timoshenko beams. Some examples of applications are presented and results are compared with analytical solutions, showing good agreement.

2 B-SPLINE AND NURBS

2.1 Knot vector

Knot vector is a set of non-decreasing ordinates of the parametric space from which B-splines are generated. A knot vector is given by $\Xi=\left\{\xi_1,\xi_2,...,\xi_{n+p+1}\right\}$, in which $\xi_i \in \mathbb{R}$ corresponds to the *i*-th knot, *i* is the knot index, *p* is the polynomial order of the B-spline, and *n* is the number of the B-spline basis functions.

A knot vector is said to be uniform when the knots are equally spaced and non-uniform, otherwise. The knots also may be repeated, and a knot vector is said to be open if the first and last knots appear *p*+1 times. An interesting feature of open knot vectors is that the basis functions generated from them are interpolatory at the ends of the parametric space interval $\left[\xi_1, \xi_{n+p+1}\right]$, that is, $N_{1,p}$ and $N_{n,p}$ are unitary at ξ_1 and ξ_{n+p+1}, respectively, while the other basis functions are null (see Fig. 1). This property makes the basis functions generated from open knot vectors analogous to the traditional finite element shape functions (Lagrange polynomials), that are interpolatory at the ends of the element.

2.2 B-spline basis functions

B-spline basis functions are generated recursively, starting from constant piecewise polynomials (*p*=0):

$$N_{i,0}=\begin{cases}1 & \text{if } \xi_i \le \xi < \xi_{i+1}, \\ 0 & \text{otherwise.}\end{cases} \tag{1}$$

Then, basis functions of order $p \geq 1$ are generated from a linear combination of two (*p*-1)-order basis functions:

$$N_{i,\mathrm{p}}\left(\xi\right)=\frac{\xi-\xi_i}{\xi_{i+p}-\xi_i}N_{i,p-1}\left(\xi\right)+\frac{\xi_{i+p+1}-\xi}{\xi_{i+p+1}-\xi_{i+1}}N_{i+1,p-1}\left(\xi\right). \tag{2}$$

If there are no repeated knots, *p*-order basis functions have *p*-1 continuous derivatives. If an internal knot appears *k* times, the number of continuous derivatives is decreased by *k*-1. When the multiplicity of the knot is equal to *p*, the basis functions are interpolatory at the ordinate of this internal knot.

Proceedings of the XXXVIII Iberian Latin-American Congress on Computational Methods in Engineering
P.O. Faria, R.H. Lopez, L.F.F. Miguel, W.J.S. Gomes, M. Noronha (Editores), ABMEC, Florianópolis, SC, Brazil, November 5-8, 2017.

Figure 1 illustrates an example of a quadratic basis generated, with dimension $n = 8$, from a non-uniform open knot vector defined by $\Xi = \{0, 0, 0, 1, 2, 3, 3, 4, 5, 5, 5\}$. Since the knot vector is open and the multiplicity of knot 3 is equal to the order of the basis, the B-spline basis functions are interpolatory at the ends of the parametric space interval $[0,5]$ and at the ordinate 3.

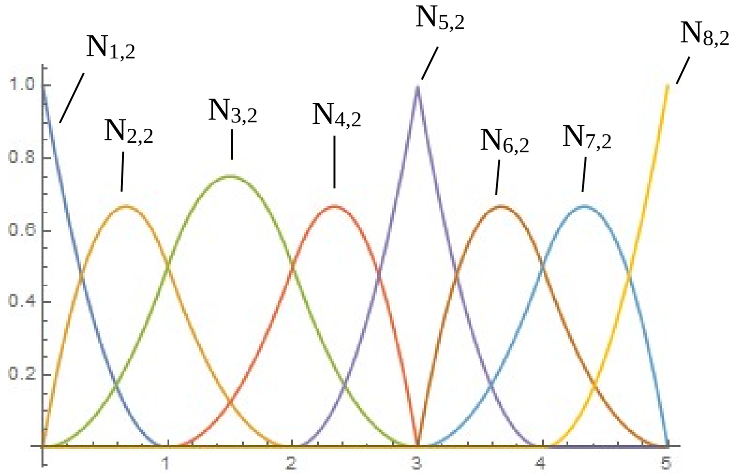

Figure 1. Quadratic B-spline basis functions obtained with Ξ = {0, 0, 0, 1, 2, 3, 3, 4, 5, 5, 5}

2.3 B-spline curve

Curves are generated from the linear combination between the B-spline basis functions and the coefficients called control points, according to the following equation:

$$S(\xi) = \sum_{i=1}^{n} N_{i,p}(\xi).C_i \tag{3}$$

Figure 2 illustrates a curve originated by the combination between the basis functions presented in Figure 1 and the set of control points C={(0,0),(0,2),(1.5,-1),(2.5,-1),(3,-1),(3.5,0),(4,0)} contained in $\mathbb{R}^2$. It is interesting to observe the discontinuity of the first derivative of the curve, with respect to ξ, evidenced by the abrupt change in orientation of its tangent direction at the control point C_5. This fact is due to the repeated knot 3, which promotes the construction of basis functions with discontinuous derivatives.

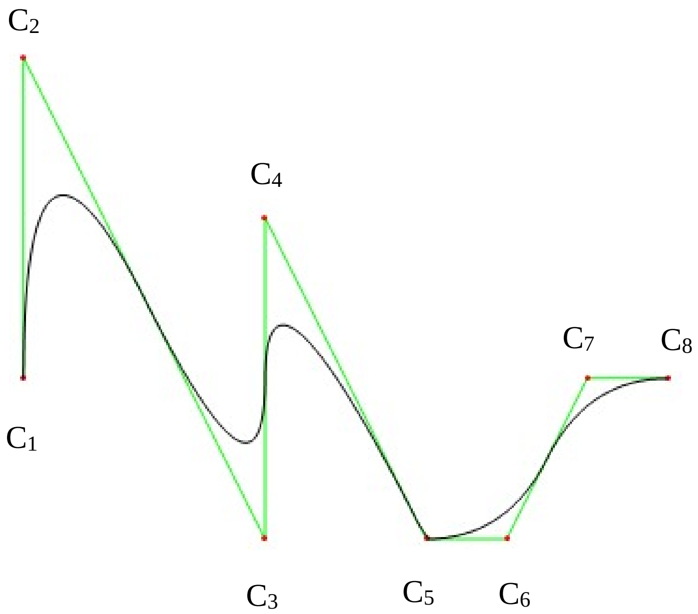

Figure 2. B-spline curve obtained with Ξ = {0, 0, 0, 1, 2, 3, 3, 4, 5, 5, 5}

2.4 Refinements h, p, k

In Isogeometric analysis, there are two kinds of refinements that are analogous with the traditional finite element method, h- and p-refinements, and a third one called k-refinement that only belongs to isogeometric analysis. The h-refinement consists in inserting knots into the knot vector, and, in p-refinement, the order of the basis functions is elevated. The k-refinement consists of order elevation followed by knot insertion and takes advantage of the non-commutativity of both to obtain a higher continuity of the basis functions. Further information about refinements can be found in Hughes *et al.* (2005) and Piegl *et al.* (1997).

2.5 NURBS

A NURBS curve is defined by:

$$S(\xi)=\frac{\sum_{i=1}^{n} N_{i,p}(\xi)\, w_i\, C_i}{\sum_{i=1}^{n} N_{i,p}(\xi)\, w_i} \tag{4}$$

Where $\{C_i\}$ are the control points, $\{w_i\}$ are the weights, and $\{N_{i,p}\}$ are the B-spline basis functions defined by an open knot vector.

The rational basis functions are given by:

$$R_{i,p}(\xi)=\frac{N_{i,p}(\xi)\, w_i}{\sum_{j=1}^{n} N_{j,p}(\xi)\, w_j} \tag{5}$$

So, Eq. (4) can be rewritten as:

$$S(\xi) = \sum_{i=1}^{n} R_{i,p}(\xi)\, C_i \tag{6}$$

An important property of NURBS, in comparison with B-splines, lies in the better flexibility in the local shape control due to the presence of the weights (w_i). Figure 3 illustrates an example of the effect of the change in weight w_2 of the B-Spline curve of Fig. 2, which corresponds to a particular case of NURBS ($w_i = 1, 1 \le i \le n$). The red and blue dashed curves correspond, respectively, to the curves with com $w_2 = 1.1$ e $w_2 = 0.9$. One can observe that elevating the weight w_2, the curve approaches the control point C_2, and vice versa.

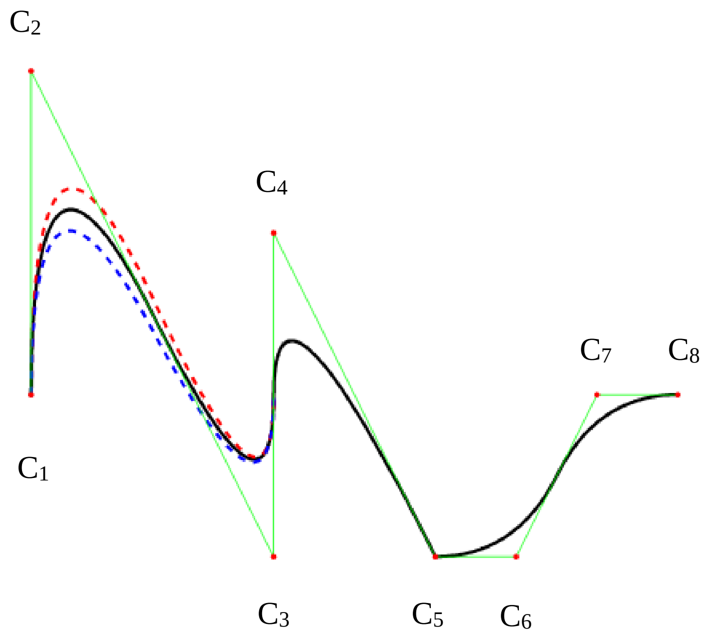

Figure 3. Example of the effect of the change in one of the weights of a NURBS curve.

3 ISOGEOMETRIC BEAM MODELS

3.1 Bernoulli-Euler beam

The first beam model presented in this paper corresponds to the Bernoulli-Euler model, whose assumptions are as follows (Bucalem *et al.*, 2011):

- Geometry: constant cross section, curved axis and the plane xz is a plane of symmetry. The coordinate s corresponds to the length of the beam axis, which passes through the centroid of the cross sections. The local axes x and z are tangential and perpendicular to the beam axis, respectively. Global axis are defined as x_1 and x_2 (see Fig. 4).

- Kinematics: cross sections remain plane and orthogonal to the deformed beam axis.

- External loading: the loads are transverse and tangential to the beam axis.

- Boundary conditions: The model allows the prescription of surface tractions and displacements in the extreme sections of the bar. On the lateral surface, the surface tractions are zero.

- Stresses: The normal stress τ_{xx} and the transverse shear stress τ_{xz} are the only nonzero stress components (due to kinematics assumption τ_{xz} also will be null, due to associated plane null distortion).

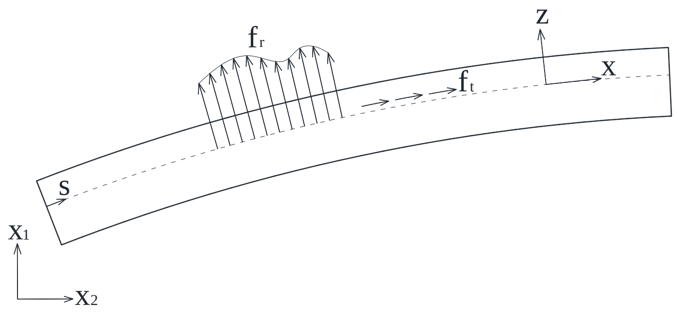

Figure 4. Curved beam model with transvers and tagential loads

Based on these assumptions and Fig. 5, the strain in the tangential direction at the bar axis, ε_{xx0}, is given by:

$$\varepsilon_{xx0} = \frac{ds^d - ds}{ds} \tag{7}$$

$$ds^d = \left(r + w\right) d\theta + du \tag{8}$$

$$\varepsilon_{xx0} = \frac{du}{ds} + \frac{w}{r} \tag{9}$$

So, the strain in the tangential direction of a point located at the distance *z* from the axis of the beam corresponds to:

$$\varepsilon_{xx} = \varepsilon_{xx0} - z\chi \tag{10}$$

Where χ is the curvature change of the beam, which is given by:

$$\chi = \frac{d}{ds}\left(\frac{dw}{ds} - \frac{u}{r}\right) \tag{11}$$

As the beam has an initial curvature (radius *r*), the curvature change also is a function of the axial displacement.

Proceedings of the XXXVIII Iberian Latin-American Congress on Computational Methods in Engineering
P.O. Faria, R.H. Lopez, L.F.F. Miguel, W.J.S. Gomes, M. Noronha (Editores), ABMEC, Florianópolis, SC, Brazil, November 5-8, 2017.

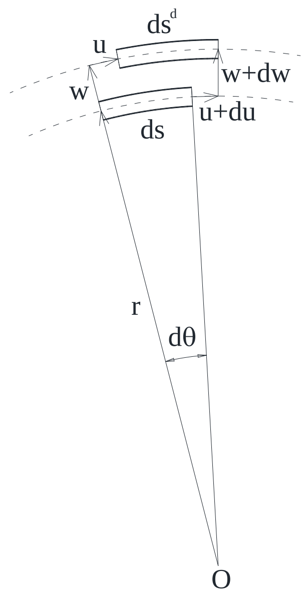

Figure 5. Longitudinal deformation of the beam axis

The formulation of the isogeometric beam element starts from the Principle of the Virtual Work:

$$\delta W_i = \delta W_e \tag{12}$$

Where δW_i and δW_e are the internal and external virtual works, respectively, and $\delta(\ )$ refers to a virtual quantity.

The internal virtual work is given by:

$$\delta W_i = \int_V \left(\tau_{xx}\delta\varepsilon_{xx}\right) dV = \int_V \left(E\left(\varepsilon_{xx0} - z\chi\right)\left(\delta\varepsilon_{xx0} - z\,\delta\chi\right)\right) dV$$

$$\delta W_i = \int_L \left(\int_A E\left(\varepsilon_{xx0}\delta\varepsilon_{xx0} - \varepsilon_{xx0}\, z\,\delta\chi - z\chi\,\delta\varepsilon_{xx0} + z^2\chi\,\delta\chi\right) dA \right) ds \tag{13}$$

As the axis passes through the centroids of the successive cross sections, one may state that:

$$\int_A z\, dA = 0 .$$

The moment of inertia is given by

$$\int_A z^2\, dA = I .$$

$$\delta W_i = \int_L \left(EA\varepsilon_{xx0}\delta\varepsilon_{xx0} + EI\,\chi\,\delta\chi \right) ds \tag{14}$$

$$\delta W_{i,N} = \int_L EA\varepsilon_{xx0}\delta\varepsilon_{xx0} ds \tag{15}$$

$$\delta W_{i,M} = \int_L EI\,\chi\,\delta\chi ds \tag{16}$$

The external virtual work is given by :

$$\begin{aligned} \delta W_e &= \int_L f_r\,\delta w\,ds + \int_L f_t\,\delta u\,ds + F_{r0}\,\delta w_0 + F_{rL}\,\delta w_L \\ &+ F_{t0}\,\delta u_0 + F_{tL}\,\delta u_L + M_0\,\delta\beta_0 + M_L\,\delta\beta_L \end{aligned} \tag{17}$$

Where f_r and f_t are the transverse and the tangential loads on the bar, respectively; F_{r0} and F_{rL} are the transverse forces applied at the ends of the bar; F_{t0} and F_{tL} are the tangential forces applied at the ends of the bar; M_0 and M_L are the bending moments applied at the ends of the bar.

Then, the transverse and axial displacements of the element are approximated using B-spline or NURBS basis functions and Galerkin's theorem is applied, which consists in defining the virtual displacements using the same functions that interpolate the real displacements (Bathe, 1996).

Transverse displacement:

$$w(\xi) = \boldsymbol{N}\,\boldsymbol{w} \tag{18}$$

$$\boldsymbol{N} = \left[N_1\, N_2 \ldots N_i \ldots N_n \right] \tag{19}$$

$$\boldsymbol{w} = \left[w_1\, w_2 \ldots w_i \ldots w_n \right]^T \tag{20}$$

$$\begin{cases} s = s(\xi) \\ \dfrac{ds}{d\xi} = J \qquad \Rightarrow \qquad \dfrac{dw}{ds} = \dfrac{1}{J}\dfrac{dw}{d\xi} \\ \dfrac{dw}{d\xi} = \dfrac{dw}{ds}\dfrac{ds}{d\xi} \end{cases} \tag{21}$$

$$\frac{d^2 w(s)}{ds^2} = \frac{1}{J^2}\frac{d^2 w(\xi)}{d\xi^2} = J^{-2}\frac{d\boldsymbol{N}^2}{d\xi^2}\boldsymbol{w} = J^{-2}\boldsymbol{N}''\boldsymbol{w} \tag{22}$$

Where ξ is the parametric space coordinate, N_i are the B-Splines or NURBS basis functions, w_i are the coefficients (generalized coordinates) associated to each function and J is the Jacobian of transformation between coordinates s and ξ.

Analogously, for the transverse virtual displacement, real and virtual axial displacements one may write:

$$\delta w(\xi) = \boldsymbol{N}\,\boldsymbol{\delta w} \tag{23}$$

$$u(\xi) = \boldsymbol{N}\,\boldsymbol{u} \tag{24}$$

$$\delta u(\xi) = \boldsymbol{N}\,\boldsymbol{\delta u} \tag{25}$$

Substituting (18), (23), (24) and (25) into (15) yields:

$$\delta W_{i,N} = \int_{\xi_1}^{\xi_{n+p+1}} EA\left(J^{-1}\boldsymbol{N}'\boldsymbol{u} + r^{-1}\boldsymbol{N}\boldsymbol{w}\right)\left(J^{-1}\boldsymbol{N}'\boldsymbol{\delta u} + r^{-1}\boldsymbol{N}\boldsymbol{\delta w}\right)Jd\xi$$

$$\begin{aligned}\delta W_{i,N} &= \int_{\xi_1}^{\xi_{n+p+1}} EA\left(J^{-1}\boldsymbol{\delta u}^T\boldsymbol{N}'^T\boldsymbol{N}'\boldsymbol{u} + r^{-1}\boldsymbol{\delta w}^T\boldsymbol{N}^T\boldsymbol{N}'\boldsymbol{u}\right)d\xi \\ &+\int_{\xi_1}^{\xi_{n+p+1}} EA\left(r^{-1}\boldsymbol{\delta u}^T\boldsymbol{N}'^T\boldsymbol{N}\boldsymbol{w} + r^{-2}J\boldsymbol{\delta w}^T\boldsymbol{N}^T\boldsymbol{N}\boldsymbol{w}\right)d\xi\end{aligned} \tag{26}$$

Substituting (18), (23), (24) and (25) into (16) yields:

$$\delta W_{i,M} = \int_{\xi_1}^{\xi_{n+p+1}} EI\left(J^{-2}\boldsymbol{N}''\boldsymbol{w} - r^{-1}J^{-1}\boldsymbol{N}'\boldsymbol{u}\right)\left(J^{-2}\boldsymbol{N}''\boldsymbol{\delta w} - r^{-1}J^{-1}\boldsymbol{N}'\boldsymbol{\delta u}\right)Jd\xi$$

$$\begin{aligned}\delta W_{i,M} &= \int_{\xi_1}^{\xi_{n+p+1}} EI\left(J^{-3}\boldsymbol{\delta w}^T\boldsymbol{N}''^T\boldsymbol{N}''\boldsymbol{w} - r^{-1}J^{-2}\boldsymbol{\delta u}^T\boldsymbol{N}'^T\boldsymbol{N}''\boldsymbol{w}\right)d\xi \\ &+\int_{\xi_1}^{\xi_{n+p+1}} EI\left(-r^{-1}J^{-2}\boldsymbol{\delta w}^T\boldsymbol{N}''^T\boldsymbol{N}'\boldsymbol{u} + r^{-2}J^{-1}\boldsymbol{\delta u}^T\boldsymbol{N}'^T\boldsymbol{N}'\boldsymbol{u}\right)d\xi\end{aligned} \tag{27}$$

Defining

$$\boldsymbol{a} = \begin{bmatrix}\boldsymbol{u}\\ \boldsymbol{w}\end{bmatrix} \tag{28}$$

$$\boldsymbol{\delta a} = \begin{bmatrix}\boldsymbol{\delta u}\\ \boldsymbol{\delta w}\end{bmatrix} \tag{29}$$

And substituting (28) and (29) into (26) and (27), we have that:

$$\delta W_{i,N} = \boldsymbol{\delta a}^T\left(\int_{\xi_1}^{\xi_{n+p+1}} EA\begin{bmatrix}J^{-1}\boldsymbol{N}'^T\boldsymbol{N}' & r^{-1}\boldsymbol{N}'^T\boldsymbol{N}\\ r^{-1}\boldsymbol{N}^T\boldsymbol{N}' & r^{-2}J\boldsymbol{N}^T\boldsymbol{N}\end{bmatrix}d\xi\right)\boldsymbol{a} \tag{30}$$

Proceedings of the XXXVIII Iberian Latin-American Congress on Computational Methods in Engineering
P.O. Faria, R.H. Lopez, L.F.F. Miguel, W.J.S. Gomes, M. Noronha (Editores), ABMEC, Florianópolis, SC, Brazil, November 5-8, 2017.

$$\delta W_{i,M} = \boldsymbol{\delta a}^T \left(\int_{\xi_1}^{\xi_{n+p+1}} EI \begin{bmatrix} r^{-2} J^{-1} \boldsymbol{N}'^T \boldsymbol{N}' & -r^{-1} J^{-2} \boldsymbol{N}'^T \boldsymbol{N}'' \\ -r^{-1} J^{-2} \boldsymbol{N}''^T \boldsymbol{N}' & J^{-3} \boldsymbol{N}''^T \boldsymbol{N}'' \end{bmatrix} d\xi \right) \boldsymbol{a} \tag{31}$$

Substituting (18), (23), (24) and (25) into (17) yields:

$$\delta W_e = \int_{\xi_1}^{\xi_{n+p+1}} f_r \, \boldsymbol{N \delta w} \, J d\xi + \int_{\xi_1}^{\xi_{n+p+1}} f_t \, \boldsymbol{N \delta u} \, J d\xi + F_{r0} \, \boldsymbol{N}(\xi_1) \boldsymbol{\delta w} + F_{rL} \, \boldsymbol{N}(\xi_{n+p+1}) \boldsymbol{\delta w}$$
$$+ F_{t0} \, \boldsymbol{N}(\xi_1) \boldsymbol{\delta u} + F_{tL} \, \boldsymbol{N}(\xi_{n+p+1}) \boldsymbol{\delta u} + M_0 \left(J^{-1} \boldsymbol{N}'(\xi_1) \boldsymbol{\delta w} - r^{-1} \boldsymbol{N}(\xi_1) \boldsymbol{\delta u} \right)$$
$$+ M_L \left(J^{-1} \boldsymbol{N}'(\xi_{n+p+1}) \boldsymbol{\delta w} - r^{-1} \boldsymbol{N}(\xi_{n+p+1}) \boldsymbol{\delta u} \right)$$

$$\begin{aligned} \delta W_e = & \int_{\xi_1}^{\xi_{n+p+1}} f_r \, J \, \boldsymbol{\delta w}^T \boldsymbol{N}^T \, d\xi + \int_{\xi_1}^{\xi_{n+p+1}} f_t \, J \, \boldsymbol{\delta u}^T \boldsymbol{N}^T d\xi + F_{r0} \, \boldsymbol{\delta w}^T \boldsymbol{N}(\xi_1)^T \\ & + F_{rL} \boldsymbol{\delta w}^T \boldsymbol{N}(\xi_{n+p+1})^T + F_{t0} \, \boldsymbol{\delta u}^T \boldsymbol{N}(\xi_1)^T + F_{tL} \, \boldsymbol{\delta u}^T \boldsymbol{N}(\xi_{n+p+1})^T \\ & + M_0 \left(\boldsymbol{\delta w}^T J^{-1} \boldsymbol{N}'(\xi_1)^T - r^{-1} \boldsymbol{\delta u}^T \boldsymbol{N}(\xi_1)^T \right) + M_L \left(\boldsymbol{\delta w}^T J^{-1} \boldsymbol{N}'(\xi_{n+p+1})^T - r^{-1} \boldsymbol{\delta u}^T \boldsymbol{N}(\xi_{n+p+1})^T \right) \end{aligned} \tag{32}$$

Substituting (28) and (29) into (32), we have that:

$$\begin{aligned} \delta W_e = & \boldsymbol{\delta a}^T \begin{bmatrix} \int_{\xi_1}^{\xi_{n+p+1}} f_t \, J \, \boldsymbol{N}^T d\xi + F_{t0} \, \boldsymbol{N}(\xi_1)^T + F_{tL} \, \boldsymbol{N}(\xi_{n+p+1})^T \\ \int_{\xi_1}^{\xi_{n+p+1}} f_r \, J \, \boldsymbol{N}^T \, d\xi + F_{r0} \, \boldsymbol{N}(\xi_1)^T + F_{rL} \boldsymbol{N}(\xi_{n+p+1})^T \end{bmatrix} \\ & + \boldsymbol{\delta a}^T \begin{bmatrix} -M_0 \, r^{-1} \boldsymbol{N}(\xi_1)^T - M_L r^{-1} \boldsymbol{N}(\xi_{n+p+1})^T \\ M_0 \, J^{-1} \boldsymbol{N}'(\xi_1)^T + M_L \, J^{-1} \boldsymbol{N}'(\xi_{n+p+1})^T \end{bmatrix} \end{aligned} \tag{33}$$

From the equations (30), (31) and (33), it is observed that the vector **a** corresponds to the vector of the displacements, and the stiffness matrix (**K**) and the vector of the external forces (**F**) correspond to the equations (34) and (35), respectively:

$$\begin{aligned} \boldsymbol{K} = & \int_{\xi_1}^{\xi_{n+p+1}} EA \begin{bmatrix} J^{-1} \boldsymbol{N}'^T \boldsymbol{N}' & r^{-1} \boldsymbol{N}'^T \boldsymbol{N} \\ r^{-1} \boldsymbol{N}^T \boldsymbol{N}' & r^{-2} J \boldsymbol{N}^T \boldsymbol{N} \end{bmatrix} d\xi \\ & + \int_{\xi_1}^{\xi_{n+p+1}} EI \begin{bmatrix} r^{-2} J^{-1} \boldsymbol{N}'^T \boldsymbol{N}' & -r^{-1} J^{-2} \boldsymbol{N}'^T \boldsymbol{N}'' \\ -r^{-1} J^{-2} \boldsymbol{N}''^T \boldsymbol{N}' & J^{-3} \boldsymbol{N}''^T \boldsymbol{N}'' \end{bmatrix} d\xi \end{aligned} \tag{34}$$

$$\begin{aligned} \boldsymbol{F} = & \begin{bmatrix} \int_{\xi_1}^{\xi_{n+p+1}} f_t \, J \, \boldsymbol{N}^T d\xi + F_{t0} \, \boldsymbol{N}(\xi_1)^T + F_{tL} \, \boldsymbol{N}(\xi_{n+p+1})^T \\ \int_{\xi_1}^{\xi_{n+p+1}} f_r \, J \, \boldsymbol{N}^T \, d\xi + F_{r0} \, \boldsymbol{N}(\xi_1)^T + F_{rL} \boldsymbol{N}(\xi_{n+p+1})^T \end{bmatrix} \\ & + \begin{bmatrix} -M_0 \, r^{-1} \boldsymbol{N}(\xi_1)^T - M_L r^{-1} \boldsymbol{N}(\xi_{n+p+1})^T \\ M_0 \, J^{-1} \boldsymbol{N}'(\xi_1)^T + M_L \, J^{-1} \boldsymbol{N}'(\xi_{n+p+1})^T \end{bmatrix} \end{aligned} \tag{35}$$

According to Cazzani *et al.* (2015), the radius of curvature of the beam and the Jacobian of transformation between s and ξ can be determined by the equations (36) and (37), respectively:

$$J = \frac{ds}{d\xi} = \sqrt{\left(\frac{ds_1}{d\xi}\right)^2 + \left(\frac{ds_2}{d\xi}\right)^2} \tag{36}$$

$$r = \frac{J^3}{\left|\frac{ds_1}{d\xi}\frac{d^2 s_2}{d\xi^2} - \frac{d^2 s_1}{d\xi^2}\frac{ds_2}{d\xi}\right|} \tag{37}$$

Where s_1 e s_2: correspond to the projections of s in x_1 e x_2, respectively ($s = s(s_1, s_2)$).

3.2 Timoshenko beam

For the Timoshenko beam model, the same assumptions of the Bernoulli-Euler beam model described in Section 3.1 are made, except for the kinematic hypothesis, since in the Timoshenko model the cross-sections remain plane, but not necessarily orthogonal to the deformed beam axis. Thus, the illustration of the global and local axes and loads of the Timoshenko beam also correspond to Fig. 4. From these hypotheses, it is possible to construct the equations presented below.

The strain in the tangential direction at the bar axis, ε_{xx0}, is given by:

$$\varepsilon_{xx0} = \frac{du}{ds} + \frac{w}{r} \tag{38}$$

So, the strain in the tangential direction of a point located at the distance z from the axis of the beam corresponds to:

$$\varepsilon_{xx} = \varepsilon_{xx0} - z\chi \tag{39}$$

Now the curvature of the axis is no more used to compound a contribution to axial strains, but the variation of the rotation angle β, when looking at successive cross sections, as follows:

$$\chi = \frac{d\beta(s)}{ds} \tag{40}$$

The shear strain is given by:

$$\gamma_{xz} = \frac{\partial u}{\partial z} + \frac{\partial w}{\partial x} = \frac{dw}{ds} - \frac{u}{r} - \beta \tag{41}$$

The formulation of the isogeometric beam element starts from the Principle of the Virtual Work:

$$\delta W_i = \delta W_e \tag{42}$$

The internal virtual work is given by:

$$\delta W_i = \int_V \left(\tau_{xx} \delta \varepsilon_{xx} + \tau_{xz} \delta \gamma_{xz} \right) dV$$

$$\delta W_i = \int_L \left(EA \varepsilon_{xx0} \delta \varepsilon_{xx0} + EI \chi \, \delta \chi + K_s GA \gamma_{xz} \delta \gamma_{xz} \right) ds \tag{43}$$

$$\delta W_{i,N} = \int_L EA \varepsilon_{xx0} \delta \varepsilon_{xx0} ds \tag{44}$$

$$\delta W_{i,M} = \int_L EI \chi \, \delta \chi ds \tag{45}$$

$$\delta W_{i,s} = \int_L K_s GA \gamma_{xz} \delta \gamma_{xz} ds \tag{46}$$

The external work is given by :

$$\begin{aligned} \delta W_e &= \int_L f_r \, \delta w \, ds + \int_L f_t \, \delta u \, ds + F_{r0} \, \delta w_0 + F_{rL} \, \delta w_L \\ &+ F_{t0} \, \delta u_0 + F_{tL} \, \delta u_L + M_0 \, \delta \beta_0 + M_L \, \delta \beta_L \end{aligned} \tag{47}$$

Then, the transverse and axial displacements of the element and the rotation of the cross sections are approximated using B-spline or NURBS basis functions, and Galerkin's theorem is applied, which consists in defining the virtual displacements using the same functions that interpolate the real displacements (Bathe, 1996).

$$\begin{aligned} & w(\xi) = \boldsymbol{N}\, \boldsymbol{w} && \delta w(\xi) = \boldsymbol{N}\, \boldsymbol{\delta w} \\ & u(\xi) = \boldsymbol{N}\, \boldsymbol{w} && \delta u(\xi) = \boldsymbol{N}\, \boldsymbol{\delta u} \\ & \beta(\xi) = \boldsymbol{N}\, \boldsymbol{w} && \delta u(\xi) = \boldsymbol{N}\, \boldsymbol{\delta \beta} \end{aligned} \tag{48}$$

Substituting (48) into (44), (45) and (46) , we have that:

$$\begin{aligned} \delta W_{i,N} &= \int_{\xi_1}^{\xi_{n+p+1}} EA \Big(J^{-1} \boldsymbol{\delta u}^T \boldsymbol{N}'^T \boldsymbol{N}' \boldsymbol{u} + r^{-1} \boldsymbol{\delta w}^T \boldsymbol{N}^T \boldsymbol{N}' \boldsymbol{u} \Big) d\xi \\ &+ \int_{\xi_1}^{\xi_{n+p+1}} EA \Big(r^{-1} \boldsymbol{\delta u}^T \boldsymbol{N}'^T \boldsymbol{N w} + r^{-2} J \boldsymbol{\delta w}^T \boldsymbol{N}^T \boldsymbol{N w} \Big) d\xi \end{aligned} \tag{49}$$

$$\delta W_{i,M} = \int_{\xi_1}^{\xi_{n+p+1}} EIJ^{-1} \boldsymbol{\delta\beta}^T \boldsymbol{N}'^T \boldsymbol{N}' \boldsymbol{\beta} d\xi \tag{50}$$

$$\begin{aligned}\delta W_{i,s} &= \int_{\xi_1}^{\xi_{n+p+1}} K_s GA\left(J^{-1}\boldsymbol{\delta w}^T \boldsymbol{N}'^T \boldsymbol{N}' \boldsymbol{w} - r^{-1}\boldsymbol{\delta u}^T \boldsymbol{N}^T \boldsymbol{N}' \boldsymbol{w} - \boldsymbol{\delta\beta}^T \boldsymbol{N}^T \boldsymbol{N}' \boldsymbol{w} \right) d\xi \\ &+ \int_{\xi_1}^{\xi_{n+p+1}} K_s GA\left(-r^{-1}\boldsymbol{\delta w}^T \boldsymbol{N}'^T \boldsymbol{N}\boldsymbol{u} + Jr^{-2}\boldsymbol{\delta u}^T \boldsymbol{N}^T \boldsymbol{N}\boldsymbol{u} + Jr^{-1}\boldsymbol{\delta\beta}^T \boldsymbol{N}^T \boldsymbol{N}\boldsymbol{u} \right) d\xi \\ &+ \int_{\xi_1}^{\xi_{n+p+1}} K_s GA\left(-\boldsymbol{\delta w}^T \boldsymbol{N}'^T \boldsymbol{N}\boldsymbol{\beta} + Jr^{-1}\boldsymbol{\delta u}^T \boldsymbol{N}^T \boldsymbol{N}\boldsymbol{\beta} + J\,\boldsymbol{\delta\beta}^T \boldsymbol{N}^T \boldsymbol{N}\boldsymbol{\beta} \right) d\xi\end{aligned} \tag{51}$$

Defining

$$\boldsymbol{a} = \begin{bmatrix} \boldsymbol{u} \\ \boldsymbol{w} \\ \boldsymbol{\beta} \end{bmatrix} \qquad \boldsymbol{\delta a} = \begin{bmatrix} \boldsymbol{\delta u} \\ \boldsymbol{\delta w} \\ \boldsymbol{\delta\beta} \end{bmatrix} \tag{52}$$

And substituting (52) into (49), (50) and (51), we have that:

$$\delta W_{i,N} = \boldsymbol{\delta a}^T \left(\int_{\xi_1}^{\xi_{n+p+1}} EA \begin{bmatrix} J^{-1}\boldsymbol{N}'^T \boldsymbol{N}' & r^{-1}\boldsymbol{N}'^T \boldsymbol{N} & \boldsymbol{0} \\ r^{-1}\boldsymbol{N}^T \boldsymbol{N}' & r^{-2}J\boldsymbol{N}^T \boldsymbol{N} & \boldsymbol{0} \\ \boldsymbol{0} & \boldsymbol{0} & \boldsymbol{0} \end{bmatrix} d\xi \right) \boldsymbol{a} \tag{53}$$

$$\delta W_{i,M} = \boldsymbol{\delta a}^T \left(\int_{\xi_1}^{\xi_{n+p+1}} EI \begin{bmatrix} \boldsymbol{0} & \boldsymbol{0} & \boldsymbol{0} \\ \boldsymbol{0} & \boldsymbol{0} & \boldsymbol{0} \\ \boldsymbol{0} & \boldsymbol{0} & J^{-1}\boldsymbol{N}'^T \boldsymbol{N}' \end{bmatrix} d\xi \right) \boldsymbol{a} \tag{54}$$

$$\delta W_{i,s} = \boldsymbol{\delta a}^T \left(\int_{\xi_1}^{\xi_{n+p+1}} K_s GA \begin{bmatrix} Jr^{-2}\boldsymbol{N}^T \boldsymbol{N} & -r^{-1}\boldsymbol{N}^T \boldsymbol{N}' & Jr^{-1}\boldsymbol{N}^T \boldsymbol{N} \\ -r^{-1}\boldsymbol{N}'^T \boldsymbol{N} & J^{-1}\boldsymbol{N}'^T \boldsymbol{N}' & -\boldsymbol{N}'^T \boldsymbol{N} \\ Jr^{-1}\boldsymbol{N}^T \boldsymbol{N} & -\boldsymbol{N}^T \boldsymbol{N}' & J\,\boldsymbol{N}^T \boldsymbol{N} \end{bmatrix} d\xi \right) \boldsymbol{a} \tag{55}$$

Substituting (48) into (47) yields:

$$\begin{aligned}\delta W_e &= \int_{\xi_1}^{\xi_{n+p+1}} f_r\, J\, \boldsymbol{\delta w}^T \boldsymbol{N}^T\, d\xi + \int_{\xi_1}^{\xi_{n+p+1}} f_t\, J\, \boldsymbol{\delta u}^T \boldsymbol{N}^T d\xi + F_{r0}\, \boldsymbol{\delta w}^T \boldsymbol{N}(\xi_1)^T \\ &+ F_{rL} \boldsymbol{\delta w}^T \boldsymbol{N}(\xi_{n+p+1})^T + F_{t0}\, \boldsymbol{\delta u}^T \boldsymbol{N}(\xi_1)^T + F_{tL}\, \boldsymbol{\delta u}^T \boldsymbol{N}(\xi_{n+p+1})^T \\ &+ M_0 \boldsymbol{\delta\beta}^T \boldsymbol{N}(\xi_1)^T + M_L \boldsymbol{\delta\beta}^T \boldsymbol{N}^T(\xi_{n+p+1})\end{aligned} \tag{56}$$

Substituting (52) into (56), we have that:

Proceedings of the XXXVIII Iberian Latin-American Congress on Computational Methods in Engineering
P.O. Faria, R.H. Lopez, L.F.F. Miguel, W.J.S. Gomes, M. Noronha (Editores), ABMEC, Florianópolis, SC, Brazil, November 5-8, 2017.

$$\delta W_e = \boldsymbol{\delta a}^T \begin{bmatrix} \int_{\xi_1}^{\xi_{n+p+1}} f_t\, J\, \boldsymbol{N}^T d\xi + F_{t0}\, \boldsymbol{N}(\xi_1)^T + F_{tL}\, \boldsymbol{N}(\xi_{n+p+1})^T \\ \int_{\xi_1}^{\xi_{n+p+1}} f_r\, J\, \boldsymbol{N}^T\, d\xi + F_{r0}\, \boldsymbol{N}(\xi_1)^T + F_{rL} \boldsymbol{N}(\xi_{n+p+1})^T \\ M_0\, \boldsymbol{N}(\xi_1)^T + M_L\, \boldsymbol{N}^T(\xi_{n+p+1}) \end{bmatrix} \tag{57}$$

From equations (53), (54), (55) and (57), one can observe that vector $\boldsymbol{a}$ corresponds to the vector of the displacements, and the stiffness matrix ($\boldsymbol{K}$) and vector of the external forces ($\boldsymbol{F}$) correspond to equations (58) and (62), respectively:

$$\boldsymbol{K} = \boldsymbol{K_N} + \boldsymbol{K_M} + \boldsymbol{K_s} \tag{58}$$

$$\boldsymbol{K_N} = \int_{\xi_1}^{\xi_{n+p+1}} EA \begin{bmatrix} J^{-1}\boldsymbol{N}'^T\boldsymbol{N}' & r^{-1}\boldsymbol{N}'^T\boldsymbol{N} & \boldsymbol{0} \\ r^{-1}\boldsymbol{N}^T\boldsymbol{N}' & r^{-2}J\boldsymbol{N}^T\boldsymbol{N} & \boldsymbol{0} \\ \boldsymbol{0} & \boldsymbol{0} & \boldsymbol{0} \end{bmatrix} d\xi \tag{59}$$

$$\boldsymbol{K_M} = \int_{\xi_1}^{\xi_{n+p+1}} EI \begin{bmatrix} \boldsymbol{0} & \boldsymbol{0} & \boldsymbol{0} \\ \boldsymbol{0} & \boldsymbol{0} & \boldsymbol{0} \\ \boldsymbol{0} & \boldsymbol{0} & J^{-1}\boldsymbol{N}'^T\boldsymbol{N}' \end{bmatrix} d\xi \tag{60}$$

$$\boldsymbol{K_s} = \int_{\xi_1}^{\xi_{n+p+1}} K_s GA \begin{bmatrix} Jr^{-2}\boldsymbol{N}^T\boldsymbol{N} & -r^{-1}\boldsymbol{N}^T\boldsymbol{N}' & Jr^{-1}\boldsymbol{N}^T\boldsymbol{N} \\ -r^{-1}\boldsymbol{N}'^T\boldsymbol{N} & J^{-1}\boldsymbol{N}'^T\boldsymbol{N}' & -\boldsymbol{N}'^T\boldsymbol{N} \\ Jr^{-1}\boldsymbol{N}^T\boldsymbol{N} & -\boldsymbol{N}^T\boldsymbol{N}' & J\,\boldsymbol{N}^T\boldsymbol{N} \end{bmatrix} d\xi \tag{61}$$

$$\boldsymbol{F} = \begin{bmatrix} \int_{\xi_1}^{\xi_{n+p+1}} f_t\, J\, \boldsymbol{N}^T d\xi + F_{t0}\, \boldsymbol{N}(\xi_1)^T + F_{tL}\, \boldsymbol{N}(\xi_{n+p+1})^T \\ \int_{\xi_1}^{\xi_{n+p+1}} f_r\, J\, \boldsymbol{N}^T\, d\xi + F_{r0}\, \boldsymbol{N}(\xi_1)^T + F_{rL} \boldsymbol{N}(\xi_{n+p+1})^T \\ M_0\, \boldsymbol{N}(\xi_1)^T + M_L\, \boldsymbol{N}^T(\xi_{n+p+1}) \end{bmatrix} \tag{62}$$

4 EXAMPLE OF APPLICATION

The example of application of the isogeometric beam models corresponds to a cantilever quarter circle arc with a transversal force applied at the free end. Figure 6 illustrates the example, and the problem data are listed below:

Proceedings of the XXXVIII Iberian Latin-American Congress on Computational Methods in Engineering
P.O. Faria, R.H. Lopez, L.F.F. Miguel, W.J.S. Gomes, M. Noronha (Editores), ABMEC, Florianópolis, SC, Brazil, November 5-8, 2017.

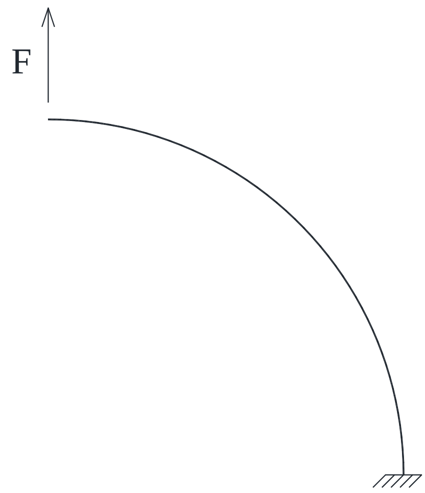

Figure 6: Example of application of curved beam models

$$b = 0{,}10\,m$$

$$h = 0{,}20\,m$$

$$K_s = 5/6$$

$$A = b\,h = 2\times10^{-2}\ m^2$$

$$I = \frac{b\,h^3}{12} = 6{,}667\times10^{-5}\ m^4$$

$$E = 2{,}4\times10^{10}\ Pa$$

$$\nu = 0{,}2$$

$$G = \frac{E}{2(1+\nu)} = 1\times10^{10}\ Pa$$

$$R = 5{,}00\,m$$

$$F = 1000\,N$$

The analytical solution for the transverse displacement at the free end for the Bernoulli-Euler beam can be found at Bucalem *et al.* (2011) and is given by:

$$w = \frac{FR}{2E}\left(\frac{R^2}{I}+\frac{1}{A}\right)cos\,\psi\left(\frac{\pi}{2}-\psi\right)$$

$$w = \frac{1000 \times 5,00}{2 \times 2,4 \times 10^{10}} \left(\frac{5,00^2}{6,667 \times 10^{-5}} + \frac{1}{2 \times 10^{-2}} \right) \times 1 \times \left(\frac{\pi}{2} \right) = 0,0614\,\mathrm{m} \tag{63}$$

For the Timoshenko beam, the analytical solution for the transverse displacement at the free end for the Bernoulli-Euler beam can be found at Cazzani *et al.* (2014) and calculated as follows:

$$c_1 = \frac{1}{2} \left(\frac{R}{EA} + \frac{R}{K_s GA} + \frac{R^3}{EI} \right) = 7,8155 \times 10^{-5}$$

$$w = F c_1 \psi \; sen \psi = 0,0614\,\mathrm{m} \tag{64}$$

The geometry of the problem can be exactly described by fourth order NURBS curve, whose control points, weights and knot vector are presented below:

Control points:

$$C = \{(5,0), (5,0.8838), (4.5580, 2.9419), (2.9419, 4.5580), (0.8838, 5), (0,5)\}$$

Weights: $p = \{1, 1, 0.9714, 0.9714, 1, 1\}$

Knot vector: $\Xi = \{0,0,0,0,0,0.5,1,1,1,1,1\}$

Then, using the above mentioned NURBS curve for the description of the geometry and its rational basis functions for interpolation of the independent variables, we arrive at the following value for the transverse displacement at the free end of the beam using software Mathematica:

Bernoulli-Euler:

$$w = 0,0565\,\mathrm{m} \tag{65}$$

Timoshenko:

$$w = 0,0570\,\mathrm{m} \tag{66}$$

Comparing the results of (63), (64), (65) and (66), there are 8,0% and 7,2% errors between the numerical solutions of the isogeometric analysis and the analytical solutions for the Bernoulli-Euler and Timoshenko models, respectively. In order to improve the accuracy of the result, the h-refinement described in Section 2.4 is performed. Thus, two knots are inserted to the knot vector, obtaining the parameters of the new NURBS curve:

Control points:

$$C_{ref} = \{(5,0), (5,0.4419), (4.8895, 1.3984), (4.3379, 2.8591),$$
$$(2.8591, 4.3379), (1.3984, 4.8895), (0.4419, 5), (0,5)\}$$

Proceedings of the XXXVIII Iberian Latin-American Congress on Computational Methods in Engineering
P.O. Faria, R.H. Lopez, L.F.F. Miguel, W.J.S. Gomes, M. Noronha (Editores), ABMEC, Florianópolis, SC, Brazil, November 5-8, 2017.

Weights: $p_{ref} = \{1, 1, 0.9929, 0.9768, 0.9768, 0.9929, 1, 1\}$

Knot vector: $\Xi_{\mathrm{ref}} = \{0, 0, 0, 0, 0, 0.25, 0.5, 0.75, 1, 1, 1, 1, 1\}$

Then, using the refined NURBS curve for the description of the geometry and the new rational basis functions for interpolation of the independent variables, we arrive at the following value for the transverse displacement at the free end of the beam through Mathematica:

Bernoulli-Euler:

$$w = 0{,}0600\,\mathrm{m} \tag{67}$$

Timoshenko:

$$w = 0{,}0612\,\mathrm{m} \tag{68}$$

Comparing the results of (63), (64), (67) and (68), 2,3% and 0,3% errors were verified between the refined numerical results of the isogeometric analysis and the analytical solutions for the Bernoulli-Euler and Timoshenko models, respectively, that is, good accuracy was obtained performing h-refinement.

5 CONCLUSION

This work presented two isogeometric curved beam models that were verified by the example of Section 4. Using only four isogeometric elements, defined by knot spans, good results were obtained, comparing with analytical solutions.

The isogeometric beam formulations were developed starting from PVW analogously to the traditional finite element method, the main difference was the use of B-Spline or rational basis functions to approximate independent variables. So, the obtained stiffness matrices and vectors of external forces are given by these basis functions.

The structure of the isogeometric models are quite similar to a finite element model, once stiffness matrix and vector of forces can be defined. Therefore, the isogeometric models can be easily implemented on existing finite element codes, by making some changes on approximation functions. Attention should be given to the integration method employed on the construction of matrices and vectors of forces, once numerical quadrature affects efficiency (Hughes *et al.*, 2008).

B-spline and NURBS-based isogeometric analysis has some advantages, such as the ease in generating the exact geometry of the model and the assurance of C^{p-1} continuity, being p the order of the spline, and besides can be easily implemented on existing finite element codes. So, it may be a viable alternative to standard Lagrange polynomial-based, finite element analysis.

ACKNOWLEDGEMENTS

The second author acknowledges CNPq (Conselho Nacional de Desenvolvimento Científico e Tecnológico) under the grant 308190/2015-7.

REFERENCES

Auricchio F, Beirão da Veiga L, Keindl J, Lovadina C, Reali A. Locking-free isogeometric collocation methods for spatial Timoshenko rods. *Computer Methods in Applied Mechanics and Engineering* 2013; **263**: 113-126.

Bathe KJ. Finite element procedures, First ed., Prentice Hall, 1996.

Beirão da Veiga L, Lovadina C, Reali A. Avoiding shear locking for the Timoshenko beam problem via isogeometric collocation methods. *Computer Methods in Applied Mechanics and Engineering* 2012; **241-244**: 38-51.

Bouclier R, Elguedj T, Combescure A. Locking-free isogeometric formulations of curved thick beams. *Computer Methods in Applied Mechanics and Engineering* 2012; **245-246**: 113-126.

Bucalem ML, Bathe KJ. The Mechanics of Solids and Strutuctures – Hierarchical Modeling and the Finite Element Solution, First ed., Springer-Verlag, New York, 2011.

Cazzani A, Malagù M, Turco E. Isogeometric analysis of plane-curved beams. *Math Mech Solids* 2014. DOI: 10.1177/1081286514531265.

Cazzani A, Malagù M, Turco E. Constitutive models for strongly curved beams in the frame of isogeometric analysis. *Math Mech Solids* 2015. DOI: 10.1177/1081286515577043.

Hughes TJR, Cottrell JA, Bazilevs Y. Isogeometric analysis: CAD, finite elements, NURBS, exact geometry, and mesh refinement. *Computer Methods in Applied Mechanics and Engineering* 2005; **194**:4135–4195.

Hughes TJR, Reali A, Sangalli G. Efficient quadrature for NURBS-based isogeometric analysis. *Computer Methods in Applied Mechanics and Engineering* 2008; **199**:301–313.

Lee SJ, Park KS. Vibrations of Timoshenko beams with isogeometric approach. *Applied Mathematical Modelling* 2013; **37**: 9174-9190.

Piegl L, Tiller W. The NURBS Book (Monographs in Visual Communication), Second ed., Springer-Verlag, New York, 1997.

Weeger O, Wever U, Simeon B. Isogeometric analysis of nonlinear Euler–Bernoulli beam vibrations. *Nonlinear Dyn* 2013. **72**: 813-835. DOI:10.1007/s11071-013-0755-5.